64th Annual Conference on Magnetism and Magnetic Materials

ABSTRACTS

AIP Publishing

IEEE MAGNETICS

Jointly sponsored by AIP Publishing, LLC and the IEEE Magnetics Society

Session FP
MAGNETICS FOR KINETIC MANIPULATION AND TRANSPORTATION (Poster Session)

Hellen Jiang, Chair
PNNL, Richland, WA, United States

FP-01. Optical Control of Diamagnetically Levitated Pyrolytic Graphite.

J. Young[1], S. Yee[1] and H. ElBidweihy[1] *1. Electrical and Computer Engineering, United States Naval Academy, Annapolis, MD, United States*

Pyrolytic graphite (PyG), when levitated above an array of alternating-pole permanent magnets, can be displaced by a localized increase in temperature due to the temperature dependence of its magnetic susceptibility. The increase in local temperature decreases the local diamagnetic forces, inducing a tilt and displacing the PyG sample in the plane of the permanent magnet array. Previous work has verified and demonstrated the optomechanical actuation of PyG using experiments and simulations [1]. Small-scale assembly methods can be extraordinarily complex processes because of the mediums in which they operate [2, 3]. This work proposes a milli-scale assembly system based on optical control of levitating diamagnetic milli-robots in air that minimizes undesirable effects such as stiction prevalent in systems with denser mediums [4]. Additionally, optical control allows accurate addressable control of multiple milli-robots able to move in close proximity to each other throughout the working surface with no work surface segmentation, a limitation of other diamagnetic control schemes [5]. A laser diode mounted on a 2-axis motorized translational stage and coupled to a controller accurately irradiates and actuates the PyG sample, which acts as a milli-robot with variable speed and acceleration. An infrared camera provides vision feedback to a MATLAB-based controller and user interface, permitting open loop or closed loop control. Figure 1 shows overlaid images providing an overview of an example trajectory of a PyG milli-robot levitating and actuated on top of an array of 6.35mm-diameter cylindrical NdFeB permanent magnets. The *x* and *y* pixel coordinates and yellow outline shown are MATLAB-generated computations of the milli-robot centroid and boundary, respectively. Figure 2 tracks the displacement of the PyG sample according to the same open loop input trajectory over a 23-second period.

[1] Miriam Ewall-Wice et al., IEEE Trans. Magn., 2019. [2] P Chen et al., Adv. Mater. 26, 2014. [3] F Xu et al., Adv. Mater. 37, 2011. [4] Z Zhakypov et al., IEEE T. Robot. 34, 2018. [5] A Hsu et al., J. Micro-Bio Robots, 2018.

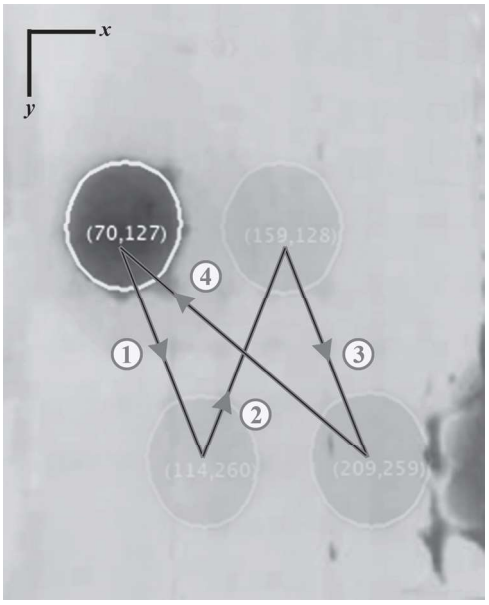

Fig. 1. Overlaid MATLAB-processed IR camera images depict an example overall trajectory of a 14mm diameter 25um thick PyG milli-robot actuated by laser irradiation.

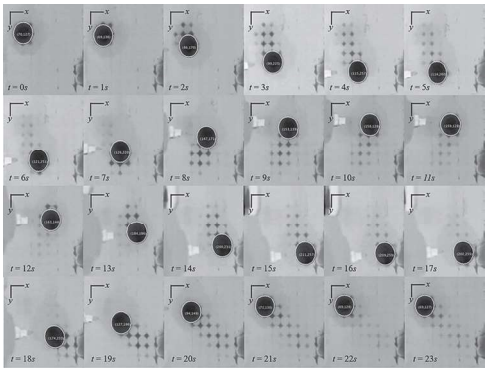

Fig. 2. IR camera images taken at one second intervals indicate the path of travel for the motion summarized by Figure 1.

FP-02. Magnetic Levitation of a Ferrofluid Droplet in Mid-Air.

T. Ohji[1], *S. Yamaguchi*[1], K. Amei[1] and K. Kiyota[1] *1. University of Toyama, Toyama, Japan*

This paper reports that the levitation of a ferrofluid droplet in the air at room temperature was realized using our magnetic levitation (maglev) device fabricated for non-contacting gripping and transport of ferrofluid droplets. The ferrofluid in a DC magnetic field theoretically deforms into an elongated spheroid in the direction of the magnetic field, as long as the surface tension of the droplet is higher than the tensile stress due to the magnetic field [1, 2]. Magnetic levitation system is suitable for experimentally verifying the

droplet deformation. Rhee et al. have reported on active magnetic levitation experiments of encapsulated ferrofluid in silicone oil [3]. The ferrofluid in the capsule floated at the steady position, but the viscous drag and buoyancy from the immiscible silicone oil slowed the capsule movement. Besides, the capsule filled with ferrofluid itself did not allow the deformation of the ferrofluid. We fabricated a new maglev system to observe the deformation and behavior of ferrofluid in an external DC magnetic field in mid-air. The maglev setup consists of an I-shaped electromagnet with a tapered magnetic pole tip, a laser displacement sensor, AD/DA, DSP, and power amplifier. The apex of a ferrofluid droplet (Base liquid: poly-alpha-olefin, viscosity: 5,000 mPa.sec, mass: 15 mg) placed on an oil-repellent film (Toyo Aluminium Inc., Toyal Ultra Lotus) was detected using the displacement sensor and actively stabilized by a PID controller. Figure 1 is a photograph of a magnetically levitated ferrofluid droplet. Figure 2 shows continuous shooting immediately before and after the levitation start with a high-speed camera (Photron Ltd., FASTCAM mini AX-50). The droplet extended upward just before leaving the oil-repellent film. After levitation, the droplet's apex fluctuated up and down for 2.5 seconds with deformation of the droplet. Finally, after 2.5 seconds, the droplet was stably levitated while keeping an oval shape of 3.4 mm height and 2.1 mm symmetrical axis length. Details of this research will appear at the conference.

[1] J. C. Bacri, et al., "Instability of ferrofluid magnetic drops under magnetic field," *J. Physique Lettres*, 43, (1982) 649-654. [2] L. D. Sherwood, "Breakup of fluid droplets in electric and magnetic fields," *J. Fluid Mech.* 188, (1988) 133-146. [3] E.J. Rhee, et al., "The position control of a capsule filled with magnetic fluid," *J. MMM*, 252, (2002) 350–352.

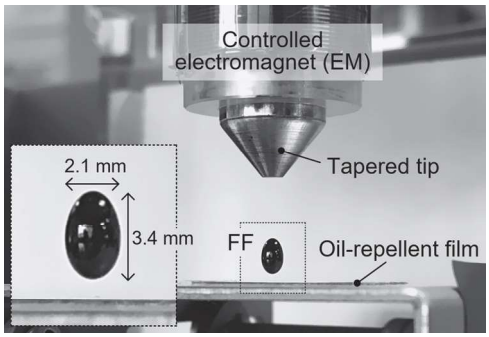

Fig. 1 Magnetically levitated ferrofluid droplet in mid-air.

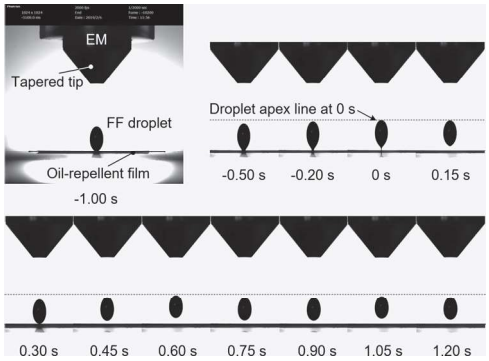

Fig. 2 Continuous shooting before and after levitation start.

FP-03. The Interaction between Two Permanent Magnets with Significantly Different Permeance Coefficients. *H. Meng*[1], Q. Wei[1], G. Tang[2], L. Cheng[3], G. Mizzell[4] and C.H. Chen[5] *1. Hangzhou Foresee Group Holding Co., LTD., Hangzhou, China; 2. Hangzhou Quadrant Technology Co. LTD, Hangzhou, China; 3. Hangzhou Magmax Technology Co., LTD., Hangzhou, China; 4. SuperMagnetMan, Pelham, AL, United States; 5. Quadrant Solutions, Louisville, KY, United States*

Even though Gauss' law for magnetic flux density (B-field) indicates there is no free magnetic charge, we can still define the effective bound magnetic charges from the magnetization of magnetic material [1]. The positive magnetic charge is what we usually called the "north pole", and correspondingly, the negative magnetic charge is what we usually called the "south pole". The interaction between the magnetic charges is governed by Coulomb's law so that like poles repel and unlike poles attract [2]. However, experiment shows that when two permanent magnets with significantly different permeance coefficients Pc (say, a small one with dimension of D4mm*4mm and Pc of 3.46, and a big one with dimension of D24mm*2mm and Pc of 0.18) were put together, with their directions of magnetization (DOM) pointing against each other, instead of repelling, they will attract to each other, especially when the coercivity of the big magnet is relatively low. This phenomenon may lead people to think that Coulomb's law for magnetic charges is not always right, and in some cases, like poles attract. In this work, we show that the above bizarre phenomenon is caused by the partial demagnetization in the low Pc magnet, rather than violation of Coulomb's law. When the experiment is carried out using sintered NdFeB magnet of N50 grade, the working point for the stand-alone low Pc magnet is very near to the knee of its demagnetizing curve, so it's very vulnerable to the external and its self-demagnetizing field. Finite Element Analysis (FEA) shows that demagnetization happens obviously in the central region of the magnet with low Pc, but the magnetization remains in the same direction all over the magnet. FEA also gives an attractive force when the above low Pc and high Pc magnets are close to each other and with opposite DOMs. Based on the magnetic charge model and Coulomb's law, the numerical integration of Coulomb's force is carried out, which gives almost the same attractive force as FEA.

[1] J. M. D. Coey, Magnetism and Magnetic Materials, 2010, Cambridge University Press, p.45. [2] Soshin Chikazumi, Physics of Ferromagnetism, second edition, 1997, Oxford University Press, p.3.

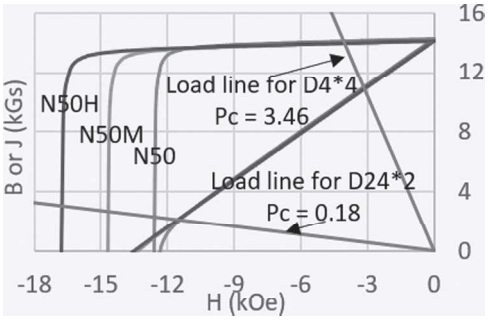

Fig.1 working point for the small and big magnets of different NdFeB grades.

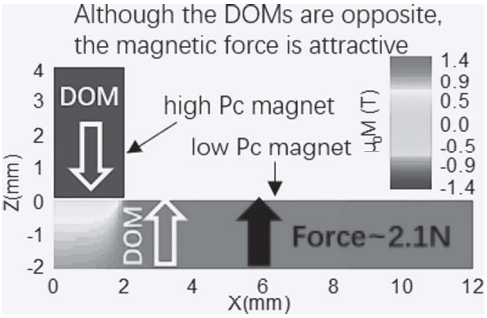

Fig.2 FEA results of magnetization distribution and magnetic force for the case of N50 NdFeB magnets. (only half of the model is shown)

FP-04. Reprogrammable Nanomagnets for Shape-morphing Micromachines. *J. Cui*[1,3], T. Huang[2], Z. Luo[1,3], P. Testa[1,3], H. Gu[2], X. Chen[2], B. Nelson[2] and L. Heyderman[1,3] *1. Laboratory for Mesoscopic Systems, ETH Zurich, Zurich, Switzerland; 2. Institute of Robotics and Intelligent Systems, ETH Zurich, Zurich, Switzerland; 3. Laboratory for Multiscale Materials Experiments, Paul Scherrer Institute, Villigen, Switzerland*

Shape-morphing micromachines have demonstrated significant potential in drug delivery, minimally invasive surgery, cell manipulation, and stenting applications [1]. With current fabrication methods, most micromachines are limited to a single type of transformation determined by their geometric design, which cannot be altered once fabricated [2]. In this work, we have developed a strategy to encode multiple shape-morphing information into transformable micromachines making use of the magnetic configurations of single-domain nanomagnet arrays. Inspired by origami, our micromachines consist of rigid panels carrying the arrays of nanomagnets separated by structured soft creases. The nanomagnets have tailored magnetic switching fields and, by applying a sequence of magnetizing fields, the arrays can be set into a particular magnetic configuration. By customizing the micromachine designs, we can obtain micromachines that perform specific shape transformations in an applied magnetic field (see Figure 1). Based on this strategy, we have built a simple four-pad micromachine with 2^4 possible magnetic configurations, demonstrating four distinct conformations when actuated by a magnetic field. Further, multicomponent micromachines were constructed by assembling modular units and, by customizing each individual unit, we have engineered a micromachine that can transform between two alphabet letters. We have also created complex folding behaviors, such as bending and twisting, and have implemented these folding modes in a microscale 'origami bird' capable of several different flapping modes. This work paves the way for the development of future intelligent microsystems that are reconfigurable and reprogrammable, which is required for biomedical applications and is also of interest for 3D magnetic and optical metamaterials. [3]

[1] B. J. Nelson, I. K. Kaliakatsos, J. J. Abbott, Microrobots for Minimally Invasive Medicine. *Annu. Rev. Biomed. Eng.* 12, 55–85 (2010). [2] M. Z. Miskin, K. J. Dorsey, B. Bircan, Y. Han, D. A. Muller, P. L. McEuen, I. Cohen, Graphene-based bimorphs for micron-sized, autonomous origami machines, *Proc. Natl. Acad. Sci.* 115, 466–470 (2018). [3] J. Cui, T.-Y. Huang, Z. Luo, P. Testa, H. Gu, X.-Z. Chen, B. J. Nelson, L. J. Heyderman, manuscript under review

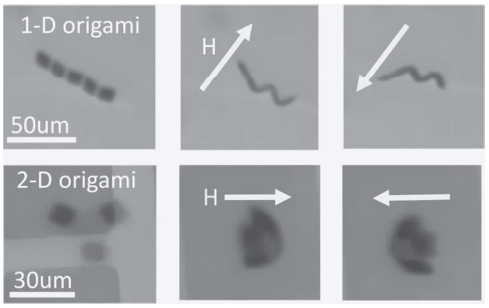

Figure 1. 1-D origami and 2-D origami micromachines demonstrate shape transformation in an applied magnetic field.

FP-05. Magnetic Control of Flexible Thermoelectric Devices Based on Macroscopic 3D Interconnected Nanowire Networks. *N. Marchal*[1], T. da Câmara Santa Clara Gomes[1], F. Abreu Araujo[1] and L. Piraux[1] *1. IMCN, Université catholique de Louvain, Louvain-la-Neuve, Belgium*

The emerging field of spin-caloritronics combines heat-driven transport with spintronics[1] and allows promising applications, such as magnetic heat valves or magnetically switchable cooling. However, dimensions in magnetic nanostructures lead to major experimental issues such as insufficient power generation capability and lack of reliable methods to obtain key spin-caloritronic parameters[2-3]. In contrast, more efficient macroscopic spin-caloritronics devices built from 3D interconnected multilayered nanowire (NW) networks (see Fig. 1) allow direct extraction of accurate key spin-caloritronics parameters[4]. They are fabricated by pulsed electrodeposition into 3D nanoporous polymer host membranes with no sample size limitation[5-7]. The branched structure of the network provides an excellent electrical connectivity, good mechanical robustness, while the pore-filled membranes show flexibility. The local removal of the gold layer serving as a cathode in the electrodeposition process yields a two-probe design suitable for magneto-transport measurements (see Fig. 2a). We studied Permalloy/copper (Py/Cu) multilayered NW networks showing giant magneto-transport (electrical, thermal and thermoelectric) properties (see Fig 2b-c), with room-temperature (RT) CPP-GMR up to 20%, and power factors comparable to that of bismuth telluride and that are magnetically modulated with magneto-power factor ratios up to 90% at RT. We observed large RT spin-dependent Seebeck coefficients of -12 μV/K. Those observations hold promise for magnetically modulated energy conversion using light and flexible thermoelectric generators and could lead to advances in future spin-caloritronic devices.

[1] G. E. W. Bauer, E. Saitoh and B. J. van Wees, *Nature Materials* 11, 391 (2012). [2] N. Liebing, *et al.*, *Phys. Rev. Lett.* 107, 177-201 (2011). [3] M. Walter, *et al.*, *Nature Materials* 10, 742 (2011). [4] T. da Câmara Santa Clara Gomes, F. Abreu Araujo and L. Piraux, *Science Advances* 5, eaav2782 (2019). [5] F. Abreu Araujo et al., *Advanced Electronic Materials* (in press). [6] T. da Câmara Santa Clara Gomes, L. Piraux, *et al.*, *Journal of Applied Physics* 120, 043904 (2016). [7] T. da Câmara Santa Clara Gomes, L. Piraux, *et al.*, *Nanoscale Research Letters* 11, 466 (2016).

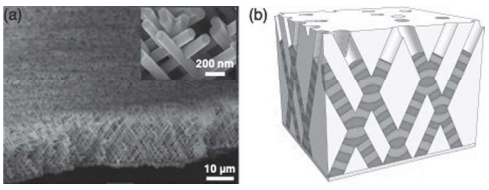

Fig. 1: (a) SEM image of a self-supported interconnected NW network film. The inset highlights the NW branched structure. (b) Schematic of the interconnected NW network with alternating magnetic and non-magnetic layers embedded within the 3D nanoporous polycarbonate template.

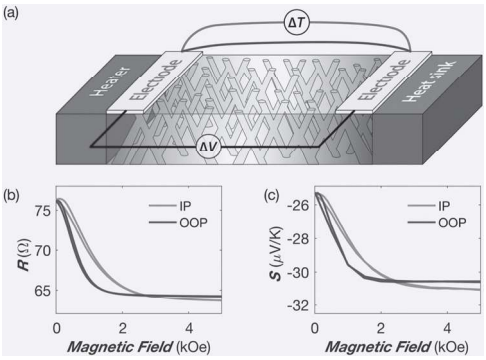

Fig. 2: (a) Device configuration for magneto-Seebeck measurements: a temperature difference ΔT between the metallic electrodes generates a thermoelectric voltage ΔV. Magnetoresistance (b) and magneto-Seebeck (c) curves for an interconnected Py/Cu NW network.

FP-06. Magnetic navigation system with a triangularly positioned triple coil set for the 2D manipulation of biomedical magnetic robots. *H. Lee*[1] and S. Jeon[1] *1. Mechanical and Automotive Engineering, Kongju National University, Cheonan, The Republic of Korea*

For 2D manipulation of biomedical small-scale magnetic robots such as in a fluid surface or a horizontal plane, conventional magnetic navigation systems (MNSs) were generally constructed with multiple numbers of 1D electromagnetic coils (Helmholtz coil, Maxwell coil, etc). However, conventional MNSs suffered from the ineffectively large overall structure, power consumption, asymmetric frequency response effect, etc [3, 4]. We propose a novel MNS simply composed of three circular coils (triple coil set, TCS), as shown in Fig.1a. Since it can be constructed with triangularly positioned identical coils, the MNS occupies minimal space to obtain a robot's working space within the system. Therefore, the corresponding power consumption and frequency response effect of the MNS can be effectively minimized during manipulation. We derived a general expression of a magnetic field generated by multiple numbers of arbitrarily positioned circular coils by using Jacobian and transformation matrices. From this expression, we could establish several constraint equations by which the proposed MNS with the TCS can selectively generate a uniform field or a gradient field near the geometric center of the coil set. Figs. 1c and 2 show several examples of the TCS's ability to generate a uniform magnetic field. Fig. 1c shows the variations of the field's uniformity and states that a TCS with a sufficiently large value of the aspect ratio can generate a more uniform field. Fig. 2 shows several cases of the uniform field generated along with the directions of 0, 45, and 90 degrees from x-axis, respectively (R/d = 1.3). We then constructed the proposed MNS, a magnetic robot, and a 2D robot manipulation environment and showed the validity of the proposed structure and manipulation method.

[1] E. Diller and M. Sitti, Found. Trends Robot., vol. 2, no. 3, pp. 143-259, 2011 [2] B. J. Nelson, I. K. Kaliakatsos, and J. J. Abbott, Annu. Rev. Biomed. Eng. 12, vol. 15, pp. 55-85, 2010 [3] S. Jeon, G. Jang, H. Choi, and S. Park, IEEE Trans. Magn., vol. 46, no. 6, pp. 1943-1946, 2010 [4] J. Nam, W. Lee, B. Jang, and G. Jang, IEEE Trans. Ind. Electron., vol. 64, no. 6, 2017

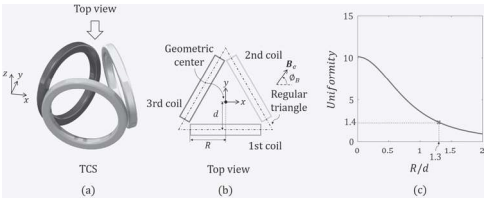

Fig. 1 (a) Schematic view of the TCS. (b) Geometric configuration of the TCS in xy-plane. (c) Variation of the field's uniformity (least square value of the Jacobian matrix) with respect to the coil's aspect ratio (R/d).

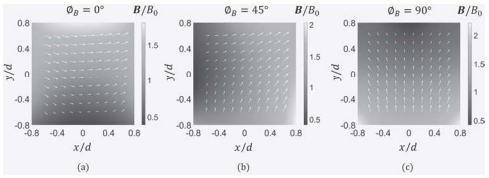

Fig. 2 Distribution of the uniform magnetic fields generated along with the directions of 0, 45, and 90 degrees from the x-axis, respectively, expressed with dimensionless values of the magnetic field and coordinate (R/d = 1.3).

FP-07. Separation of Diamagnetic and Weak Paramagnetic Solid Particles Realized by a Small Nd-Fe-B Magnetic Circuit. *C. Ueda*[1] *1. Science, Earth and Space Science, Osaka, Japan*

Most solid particles that are studied in industrial and/or basic researches are composed of diamagnetic or weak paramagnetic materials; possibilities of field-induced dynamical motions were not expected in these materials unless an ultra-strong field were applied to these particles. We were able to separate a mixture of heterogeous particles into groups of different materials for the first time using a pair of Nb-Fe-B magnetic plates, and the materials of the separated groups were immediately determined from their translating velocities; this was realized by comparing the value experimental susceptibility obtained from velocity with a list of published values [1][2]. The separation is based on a recent finding that acceleration a of particle induced by a magnetic volume force is independent to its mass [3]; it is deduced from an energy conservation law that a is uniquely determined by intrinsic susceptibility of the material. In performing a refined analysis on a mixture of heterogeneous particles, it is desirable to thoroughly separate the particles into groups of different materials before putting them to the analyses. In future, the proposed technique can realize the above task of pre-treatment, and then it may play a role of a chromatography technique, a conventional technique of pre-treatment. Extraction of rare-metal(i.e. Au, In, Ag) from the heterogeneous mixture is also possible because the susceptibilities of these materials are considerably small compared to other materials [2], A methodo separate mixture of weak magnetic particles by its concentration of paramagnetic Fe ion is newly proposed [4].

[1] Sci. Rep.6, 38431 (2016). [2] Sci. Rep.9, 3971 (2019). [3] J.PS.J. 79, 064709 (2010). [4] Adv. Mater. 1154, (2019) in print

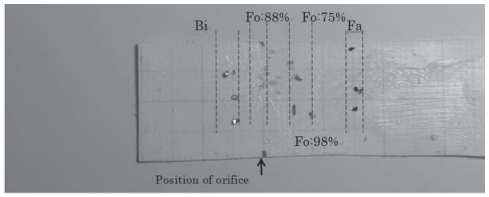

Image of a collecting sheet (cross sectional paper) observed after the experiment of magnetic separation performed in normal gravity. Sequence of the positions of the silicate samples are in the order of Fe concentrations [4].

FP-08. Optimal Design and Experimental Verification of a Linear Magnetic Gear. *S. Seo*[1], K. Shin[1], G. Jang[1], S. Kim[1] and J. Choi[1] *1. Dept. of Electrical Engineering, Chungnam National University, Daejeon, The Republic of Korea*

Electrical equipment typically cannot be driven without power transmission. For this reason, gears are used in a variety of mechanical systems [1–2]. However, mechanical gears cause mechanical losses when transmitting power. This problem has motivated various studies on magnetic gears, which can effectively compensate for the disadvantages of conventional gears [3–4]. In particular, in linear motion systems such as those used for wave power generation, utilizing a linear gear is inevitable. Thus, research on magnetic gears with tubular structures has recently been conducted.

Major limitations identified for this type of gear are manufacturing difficulties and high costs. Similar results are obtained when simplifying the tubular structure to a linear structure [5]. However, few studies related to linear magnetic gears have been conducted thus far. Therefore, this is a very relevant topic. In this study, we present an optimal design and verification of a linear magnetic gear (LMG). First, we choose a basic model that considers limitation specifications and then select an optimal model through parametric analysis. Next, an optimal model is presented considering mechanical characteristics through stress analysis. Finally, the reliability of the analysis is verified through experiments on an actual manufactured model. Fig. 1 present the structure and experimental system of the LMG. More specifically, Fig. 1(a)–(c) show the basic and two optimal shapes, respectively, of the flux-modulation poles (FMPs). Fig. 2(a) and (b) present comparisons of analytical and experimental results, and Fig. 2(c) shows stress analysis results of the optimal FMP shape. All results reveal the superiority of the optimal model design process. The final manuscript will provide more details on the design method and verification.

[1] B. Drew, A. R. Plummer, and M. N. Sahinkaya, "A review of wave energy converter technology," *in Proc. IMechE*, Part A: J. Power Energy, vol. 223, Jun. 2009, pp. 887–902. [2] I. Martins, J. Esteves, G. D. Marques, and F. P. Silva, "Permanentmagnets linear actuators applicability in automobile active suspensions," *IEEE Trans. Veh. Technol.*, vol. 55, no. 1, pp. 86–94, Jan. 2006. [3] N. W. Frank and H. A. Toliyat, "Analysis of the concentric planetary magnetic gear with strengthened stator and interior permanent magnet inner rotor," *IEEE Trans. Ind. Appl.*, vol. 47, no. 4, pp. 1652–1660, Jul.–Aug. 2011. [4] K. Atallah and D. Howe, "A novel high-performance magnetic gear," *IEEE Trans. Magn.*, vol. 37, no. 4, pp. 2844–2846, Jul. 2001. [5] S. T. Boroujeni, J. Milimonfared, and M. Ashabani, "Design, prototyping, and analysis of a novel tubular permanent-magnet linear machine," *IEEE Trans. Magn.*, vol. 45, no. 12, pp. 5405–5413, Dec. 2009.

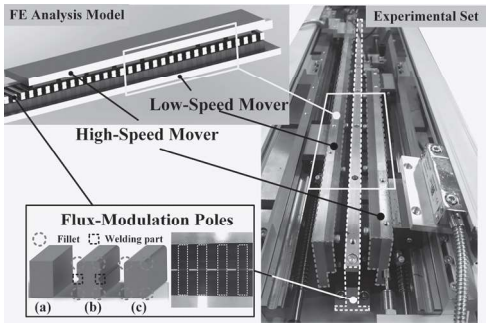

Fig. 1 Structure and experimental system of a linear magnetic gear : (a) basic model, (b) optimal model 1, (c) optimal model 2.

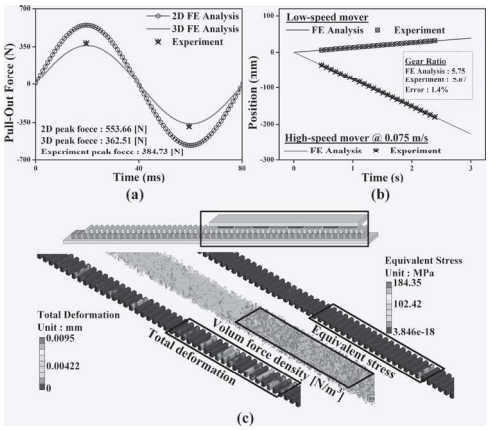

Fig. 2. Analytical results of a linear magnetic gear: (a) pull-out force comparison of optimal model 2, (b) position comparison of optimal model 2, (c) stress analysis results of flux-modulation pole of the optimal model 2.

FP-09. A Novel Five-Degree-of-Freedom AC-DC Hybrid Magnetic Bearing. *W. Zhu*[1] and Q. Le[1] *1. Huaiyin Institute of Technology, Huai'an, China*

High-speed motors have the advantages of high efficiency and power density. The high-speed motor directly drives the load, which eliminates the transmission mechanism, reduces the volume and weight of the drive system, and has no transmission loss and noise. It has broad application prospects in many fields such as aerospace, flywheel energy storage and high-speed CNC machine tools. HMB is a high-performance bearing which uses electromagnetic force to support high-speed rotor. The high-speed motor supported by HMB has many excellent qualities, such as no friction, no wear, no lubrication and sealing, no oil pollution, high speed, high precision, low noise, long life and adjustable dynamic characteristics [1]-[2]. The HMB realizes the development of the motor towards higher speed and power, and provides a new solution for the high-speed transmission system. A novel five degrees of freedom (DOFs) AC-DC HMB is proposed in this paper, whose structure is compact. Stable suspension performance can be implemented in one unit. The radial four DOFs are completely controlled by two three-phase power inverters. The axial one DOF is driven by a DC amplifier.Firstly, the structure and suspension force production mechanism are introduced. The magnetic circuits are calculated by equivalent magnetic circuit method. The mathematical models of suspension force are deduced. The main parameters of the five DOFs HMB is designed. The magnetic circuits are analyzed by the three-dimensional finite element method, and the suspension mechanism of the five DOFs is verified. The relationships between suspension forces and currents are calculated. The research results have shown that the structure of five DOFs AC-DC HMB is reasonable, and the suspension mechanism and mathematical models are correct. The 3D structure of the five-DOF AC-DC HMB is shown in Fig. 1(a). Fig. 1(b) shows the operating principle of the proposed HMB.Fig.2(a) shows the magnetic density distribution. The curve of the suspension force in the x, y and z- direction are calculated by the parametric method as shown in Fig. 2(b). The results of FEA are agree with the theoretical values.

[1] S. Chen and F. Lin, "Robust Nonsingular Terminal Sliding-Mode Control for Nonlinear Magnetic Bearing System," *IEEE Trans. Control Syst. Technol.*, vol. 19, no. 3, pp. 636-643, May 2011. [2] C. R. Morrison, M. W. Siebert and E. J. Ho, "Electromagnetic Forces in a Hybrid Magnetic-Bearing Switched-Reluctance Motor," *IEEE Trans. Magn.,* vol. 44, no. 12, pp. 4626-4638, Dec. 2008.

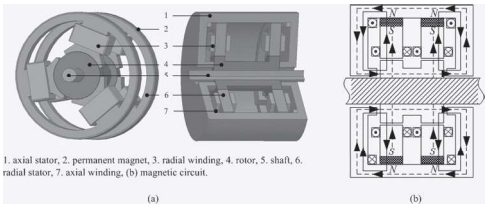

Fig. 1. 3D model and magnetic circuit

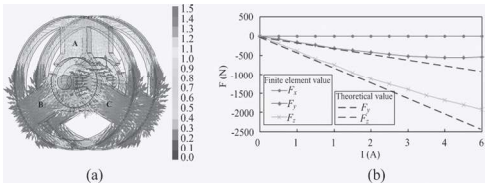

Fig. 2. Magnetic density diagram.

FP-10. Eddy Current Braking Force Analysis of an Ironless Linear Synchronous Motor with Cooling System. *L. Zhang*[1] *1. Harbin Institute of Technology, Harbin, China*

As the permanent magnet linear synchronous motor (LSM) have many advantages such as high force density, rapid dynamic response, low thermal losses, and simple structure, the linear motor drive technology is used

more and more widely in ultra-precision positioning and processing areas. However, the thrust ripple, which is the main disadvantage of permanent magnet linear synchronous motor, results in a periodic force oscillation with respect to the mover position. For the linear synchronous motor with cooling system, the eddy current braking force introduced in the cooling system is a main reason for thrust ripple. In this paper, analysis and calculation of the eddy current braking force of an ironless LSM is investigated. Fig. 1 shows the side-view of the ironless LSM which is investigated in this paper. This LSM consisting of a mover with ironless winding and a yoke with double layer Halbach magnet array mounted on it. The primary winding is divided into two layers, and the cooling system is located between the two layers. Water flowing through the cooling system and carrying the heat away. The vector magnetic potential is used to solve the magnetic system, and the differential equations are solved by the separation of variables method according to the boundary conditions. By solving the equations of the vector magnetic potential, the flux density distribution can be obtained and the expression of the eddy current density can be got furtherly. Then, the eddy current braking force introduced in the cooling system can be drived. The finite element model of the ironless LSM with cooling system is established by using Ansoft. The eddy current braking force introduced in the cooling system is calculated and compared with the analytical results. Based on the above investigation, an ironless LSM with cooling system is designed and established in laboratory as shown in Fig.2. Performance of the ironless LSM such as the detent force, eddy current braking force are measured with the prototype. And the experiment results are validated by finite element analyzed results.

[1] Ender Kazan, Ahmet Onat, "Modeling of air core permanent-magnet linear motors with a simplified nonlinear magnetic analysis," *IEEE Transactions on Magnetics*, Vol. 47, No. 6, pp. 1753-1762, Jun. 2011. [2] Changsoo Jang, Jong Young Kim, Yung Joon Kim, Jae Ok Kim, "Heat transfer analysis and simplified thermal resistance modeling of linear motor driven stages for SMT applications," *IEEE Transactions on Components and packaging TechnoloGies*, Vol. 26, No. 3, pp. 532-540, Sep. 2003.

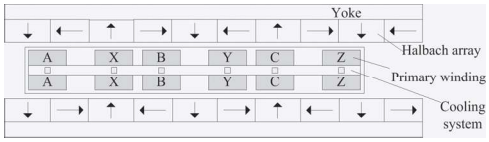

Fig. 1. The side-view of the ironless linear synchronous motor with cooling system.

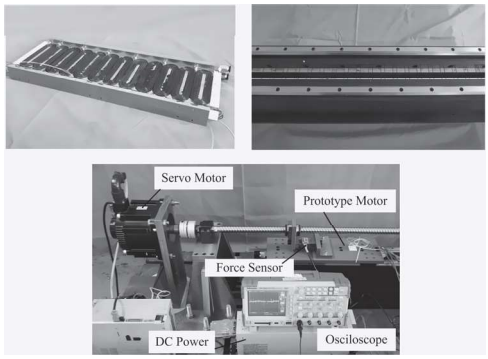

Fig. 2. The prototype motor.

FP-11. A New HTS Traveling Magnetic Electromagnetic Halbach Array for Electromagnetic Launch System. *W. Qin*[1] *1. School of Electrical Engineering, Beijing Jiaotong University, Beijing, China*

Electromagnetic launch (EML) systems need the driving sources featuring great thrust, high speed [1]. High Temperature Superconducting (HTS) has a bright future in the electromagnetic aircraft launch system for its high performance [2]–[3]. HTS windings with slotted iron core primary is the popular choices of LIM for the applications of EML[4]. The motor with slotted has a high efficiency, but its thrust ripple is high too and the core becomes saturated easily for large current carrying capacity of HTS. In this paper, a novel HTS Traveling Magnetic Electromagnetic Halbach Array (TMEHA) shown as in Fig.1 was proposed as the primary windings of the motor, of which are self-shielding, have ability for creating magnetic flux enhanced on one side (strong side) of the array while the flux cancelled on the other side (weak side) as Fig.1. The primary section for installing and fixing HTS coils is made of non-magnetic and non-conductive material, which is different from conventional iron core. HTS TMEHA successfully alleviates the saturation of the iron core and take full use of the advantages of the superconductors. The structure and the operation principle of the proposed array are described, and the major design parameters are optimized for maximum thrust force. Moreover, electromagnetic performances of different type array are compared by 3-D analytical and finite-element method. Theoretical and simulation analysis shows that the proposed array has a higher thrust and eliminates the cogging effect for heavy load EML. Finally, a 3-D modeling LIM with Electromagnetic Halbach array is built for a global observation of motor structure and further verification of the 3-D analysis. The results prove that the proposed motors can effectively satisfy the requirements of EML.

[1] M. R. Doyle, D. J. Samuel, T. Conway, and R. R. Klimowski, "Electromagnetic aircraft launch system-EMALS," IEEE Trans. Magn., vol. 31, no. 1, pp. 528–533, Jan. 1995. [2] K. Yoshida and H. Matsumoto, "Design and simulation of HTS bulk linear synchronous motor," Physica C, vol. 378-381, pp. 833–837, Oct. 2002. [3] K. Yoshida and H. Matsumoto, "Propulsion and guidance simulation of HTS bulk linear synchronous motor taking into account E–J characteristic," Phys. C, vol. 392-396, pp. 690–695, 2003. [4] J. Zhao, T. Q. Zheng, W. Zhang, J. Fang, and Y. M. Liu, "Influence analysis of structural parameters on electromagnetic properties of HTS linear induction motor," Phys. C, vol. 471, no. 21/22, pp. 1474–1478, Nov. 2011.

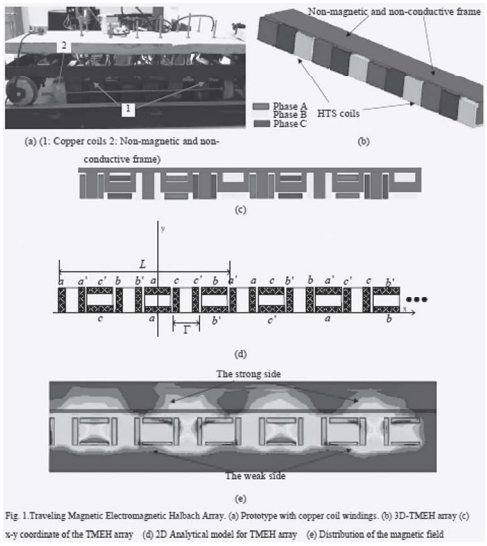

Fig. 1.Traveling Magnetic Electromagnetic Halbach Array. (a) Prototype with copper coil windings. (b) 3D-TMEH array (c) x-y coordinate of the TMEH array (d) 2D Analytical model for TMEH array (e) Distribution of the magnetic field

FP-12. A study on design feasibility through optimal design and performance test of All-In-One system using NSDLIM(Non-Symmetry Double-sided Linear Induction Motor). *K. Seo*[1], C. Park[1], J. Lee[1], T. Kim[2], H. Oh[1], J. Lim[1], w. Ji[3] and H. Lee[1] *1. Korea National University of Transportation (KNUT), Uiwang-si, The Republic of Korea; 2. University of Michigan-Dearborn, Dearborn, MI, United States; 3. Hanyang University, Seoul, The Republic of Korea*

The conventional railway uses the adhesive driving system and generates noise, vibration, dust, and abrasion due to mechanical contact, and because it travels in the air, the maximum speed is limited due to air resistance. To solve these problems, magnetic levitation trains such as hyperloop have been developed[1]. Because the Hyperloop is no mechanical friction, there requires propulsion, levitation, and guiding force for driving, and a device for generating each force is necessary. For these reasons, several countries

have used more than two devices to generate propulsion, levitation, and guidance forces of Hyperloop. However, if there are too many such devices, there is a disadvantage that maintenance and manufacturing costs increase and control is difficult. To solve these problems, recently, research of All-In-One system using NSDLIM (Non-Symmetry Double-sided Linear Induction Motor), which generates a force of propulsion, levitation, guidance in one interface has been carried out. In the study, the initial NSDLIM which travels at 1000km/h speed was designed and FEM analysis was carried out, and detailed design was carried out to achieve the required performance. In addition, the analysis of the change in the conductivity of the secondary material was carried out[2]. However, 1% conductivity of Aluminum model selected as the final performance improvement model is impossible in actual manufacturing and since the performance characteristics of the motor can not be predicted due to the repulsive magnetic field of the secondary material in high speed, Therefore, research on optimal design considering these problems is necessary and is being studied in many countries[3]. This paper is a follow-up study of the All-In-One system. The optimal design parameters of primary and secondary were selected through the FEM analysis using the reaction surface method (RSM) and the final performance improvement model was proposed. In addition, the design feasibility for the proposed final performance improvement model was verified through the performance test after manufacturing the small-scale rotary type test machine.

[1]. H. W. Lee, K. C. Kim, and J. Lee, "Review of maglev train technologies," IEEE Trans. Magn, Vol. 42, p.1917-1925 (2006) [2]. Woo-Young Ji (2018) A Study of Non-Symmetric Double-Sided Linear Induction Motor for Hyperloop All-In-One System(Propulsion, Levitation, and Guidance), IEEE Trans on Magnetics, Vol 54 (2019) [3.] G. Lv, T. Zhou, D. Zeng, Z. Liu, "Design of Ladder-Slit Secondaries and Performance Improvement of Linear Induction Motors for Urban Rail Transit", IEEE Trans. Ind. Electron, Vol. 65, p.1187-1195 (2018)

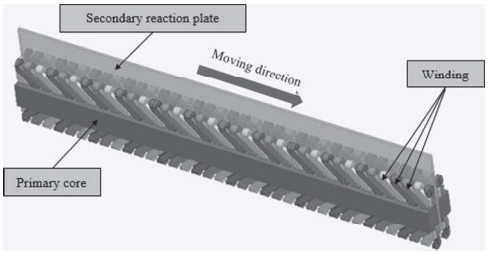

Fig. 1 Structure of NSDLIM

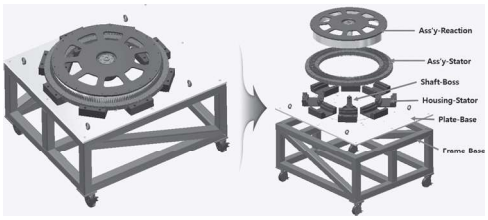

Fig. 2 Structure of small-scale rotary type test machine

FP-13. Feasibility Study on Combined Piezoelectric (Solid) and Ferrofluid (Liquid) Vibration Energy Harvester. *N. Anand*[1] and R. Gould[1] *1. Mechanical & Aerospace Engineering, North Carolina State University, Raleigh, NC, United States*

In this paper we have introduced and studied the feasibility of a hybrid solid-liquid vibration energy harvester. The energy harvester consists of a ferrofluid partially filled in a tank and a piezoelectric beam fixed at one of the tank walls. External to tank lies two powerful electromagnets which magnetize the ferrofluid non-uniformly in space, and hence creates a potential for energy harvesting due to changing magnetic field when subject to external oscillations. We used different piezoelectric beam configurations along with different oscillation loads to study and characterize this 2-D multi-scale, multiphysics and multiphase fluid structure interaction. The tank is subjected to an external oscillatory motion, which sloshes the ferrofluid and oscillates the beam by means of two modes, one due to beam's inertia and second due to the impact of the ferrofluid on the beam. An external circuit is also modelled which has a load resistor to measure the voltage generated from the piezo and from the ferrofluid sloshing. The parameters varied are the piezo beam length, beam thickness, piezo materials, ferrofluid fill height, oscillation frequency and the oscillation amplitude. The natural frequency modes for the piezoelectric beam are very important, since at those modes the beam harvests the highest power. We have observed that when the fluid motion vibrates the beam such that it is near its first natural frequency, the power harvested naturally increases. Finally, we have proposed design rules for such a system to obtain the highest performance.

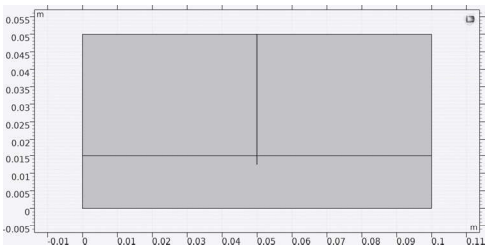

System Configuration

FP-14. Research on Multi-objective Task Scheduling Algorithm for Electromagnetic Cloud Computing. *L. Jin*[1], J. Wang[1], X. Liu[1] and W. Feng[1] *1. Tianjin Polytechnic University, Tianjin, Tianjin, China*

With the development of cloud computing in the field of high-performance computing, large-scale electromagnetic finite element and multi-sample computing are gradually completed by cloud computing. Therefore, cloud platform task scheduling has become an important issue to be solved. In this paper, a cloud resource scheduling model is constructed. Aiming at the indivisibility of electromagnetic finite element single sample computation, a multi-group hybrid genetic algorithm with particle swarm search is proposed. The approach is tested on instances taken from the literature and practical data. The computation results validate the effectiveness of the proposed algorithm. The finite element efficient calculation and the full utilization of resources are realized on the cloud platform. I. INTRODUCTION How to allocate cloud computing resources to the users of electromagnetic finite element computation under constrained conditions and achieve efficient scheduling to reduce the computing time of tasks and improve the efficient utilization of cloud computing resources has become a practical problem in the field of cloud computing[1,2]. II.Scheduling in cloud In the environment of cloud computing, different types of virtual machines with different performance characteristics are abstracted from a large number of physical resources by virtualization technology, and tasks are calculated by scheduling virtual machine resources. III.Cloud Platform Scheduling Algorithms A hybrid multi-population algorithm based on cloud platform is proposed by combining particle swarm optimization and genetic algorithm, as shown in Fig.1. IV.Conclusion Three-dimensional motors, three-dimensional inductors and TEAM Problem 7 were tested on cloud platform, and the optimal CPU core number and memory allocation in computing time and resource consumption were obtained. The sample numbers of three finite element calculation cases were 8, 4 and 4, respectively. The most satisfactory task scheduling scheme was obtained, as shown in Fig.2.

[1]Y. Zhao, and L. Chen, "Efficient task scheduling for many task computing with resource attribute selection," *China Communications*, Vol. 11, No. 12, PP. 125-140, 2014. [2]M. Mezmaz, N. Melab and D. Tuyttens, "A parallel bi-objective hybrid metaheuristic for energy-aware scheduling for cloud computing systems," *Journal of Parallel and Distributed Computing*, Vol. 71, No. 11, PP. 1497-1508, 2011.

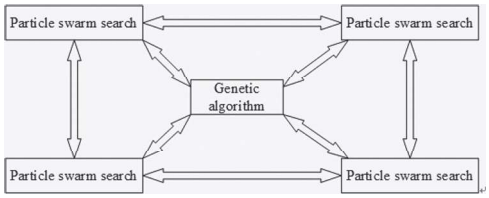

Multi-population hybrid algorithm structure diagram

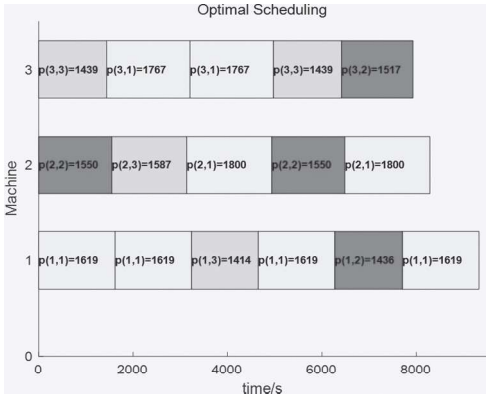

the most satisfactory scheduling scheme

FP-15. Application of Grain-Oriented Electrical Steel Used in Super-High Speed Electric Machines. *R. Pei*[1] and L. Zeng[1] *1. InnMag New Energy Ltd., Suzhou, China*

Abstract — Electrical steel is one of the core magnetic materials in Electrical Vehicle(EV) traction motor. In terms of high power density and torque density for the EV traction motors. Traditional Non Grain-Oriented (NGO) silicon steel is difficult to satisfy these requirements because of limited saturation flux density and magnetic permeability. This paper mainly presents that a novel thin anisotropic Grain-Oriented (GO) silicon steel is used in high-speed (up to 14000rpm)traction motors after deeply analysing magnetic saturation, power loss, thermal conductivity and mechanical property of a traction motor with high-frequency (50Hz-400Hz) and high-torque running status. It applies a combination design between NGO and GO steel in order to avoid the low magnetic permeability in the transverse direction. The noise and magnetostriction of the electric machine can be reduced by applying a self-stick punching technique between GO steel sheets in a stator. The research on numerical modeling and experimental results has been done. The new prototype is being fabricated and it can be produced in mass production in next few years. The measured B-H curve states the difference between NGO and GO silicon steel in the direction of magnetization can be shown in Figures. The novel prototype of high-speed traction motor has been designed with 12 slots and 8 poles. The rating/peak power is 15/30kW. According to the relationship of flux density, iron loss and offset angle of the rolling direction for GO and NGO steel, we should use the magnetic property of GO steel in the range of 0^o and 30^o of the rolling direction to design a stator. The new design can be shown in the Figures. The new design shows the power loss of the stator remarkably decrease by using GO steel. Moreover, the saturation flux density and magnetic permeability will rise. After the motor teeth adopt the grain-oriented silicon steel sheet, the efficiency of the motor rated condition increases from 96.6% to 97.8%, an increase of 1.2%.

[1]Taghavi S, Pillay P. A Novel Grain-Oriented Lamination Rotor Core Assembly for a Synchronous Reluctance Traction Motor With a Reduced Torque Ripple Algorithm[J]. IEEE Transactions on Industry Applications, 2016, 52(5):3729-3738. [2]Taghavi S, Pillay P. An innovative rotor core assembly for high performance 4-pole synchronous reluctance traction motor using grain oriented lamination[C]// Electric Machines & Drives Conference. IEEE, 2016:90-95. [3]Enomoto Y, Ito M, Koharagi H, et al. Evaluation of experimental permanent-magnet brushless motor utilizing new magnetic material for stator core teeth[J]. IEEE Transactions on Magnetics, 2005, 41(11):4304-4308.

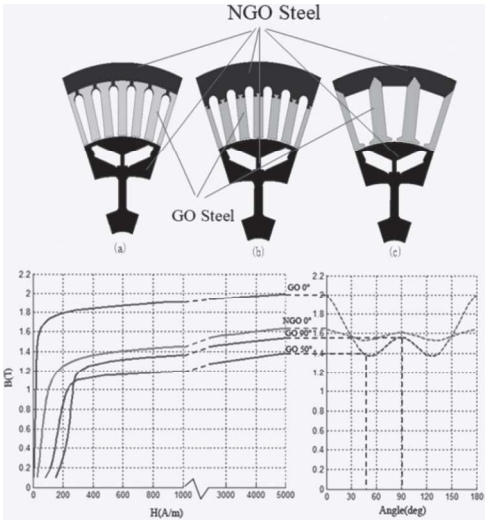

Different NGO and GO joint structures; The B-H curves between GO and NGO Silicon Steel

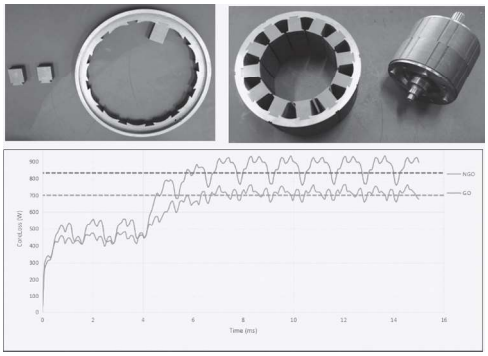

The iron core fabricated by GO and NGO; Results.